

# Superconducting/ferromagnetic diffusive bilayer with a spin-active interface: a numerical study

Audrey Cottet<sup>1</sup> and Jacob Linder<sup>2</sup>

<sup>1</sup> *Ecole Normale Supérieure, Laboratoire Pierre Aigrain,  
24 rue Lhomond, 75231 Paris Cedex 05, France and*

<sup>2</sup> *Department of Physics, Norwegian University of Science and Technology, N-7491 Trondheim, Norway*  
(Dated: October 30, 2018)

We calculate the density of states (DOS) in a diffusive superconducting/ferromagnetic bilayer with a spin-active interface. We use a self-consistent numerical treatment to make a systematic study of the effects of the Spin-Dependence of Interfacial Phase Shifts (SDIPS) on the self-consistent superconducting gap and the DOS. Strikingly, we find that the SDIPS can induce a double gap structure (DGS) in the DOS of the ferromagnet, even when the superconducting layer is much thicker than the superconducting coherence length. We thus obtain DOS curves which have interesting similarities with those of Phys. Rev. Lett. **100**, 237002 (2008).

PACS numbers: 73.23.-b, 74.20.-z, 74.50.+r

## I. INTRODUCTION

Superconducting/ferromagnetic ( $S/F$ ) hybrid structures give rise to a fascinating interplay between two antagonist electronic orders. The ferromagnetic exchange field  $E_{ex}$  privileges one spin direction while standard superconductivity favors singlet correlations. This leads to a rich behavior which has triggered an intense activity in the last years (see e.g. Refs. 1,2). In particular, the "superconducting proximity effect", i.e. the propagation of the superconducting correlations in ferromagnets, has been widely studied. This propagation is accompanied by spatial oscillations of the superconducting order parameter, because  $E_{ex}$  induces an energy shift between electrons and holes. As a result, one can build electronic devices with new functionalities, such as Josephson junctions with negative critical currents<sup>3</sup>, which could find applications in the field of superconducting circuits<sup>4,5</sup>. From a fundamental point of view, it is very instructive to study the density of states (DOS) of  $S/F$  structures. So far, this quantity has been less measured<sup>6,7,8,9,10</sup> than critical temperatures or supercurrents. However, this way of probing the superconducting proximity effect is very interesting because it provides spectroscopic information. One striking consequence of the spatial oscillations of the order parameter in the  $F$  layer is that the zero-energy DOS can become larger than in the normal state for certain ferromagnet thicknesses<sup>6</sup>.

The behavior of  $S/F$  hybrid circuits depends crucially on the properties of the interfaces between the  $S$  and  $F$  materials. In this paper, we focus on the case of diffusive structures. Diffusive  $S/F$  interfaces have been initially described with spin-independent boundary conditions<sup>11</sup>. It has been found that the amplitude of the superconducting proximity effect directly depends on the tunnel conductance  $G_T$  of an interface (see e.g. Ref. 1). Later, spin-dependent boundary conditions have been introduced, in the limit of a weakly polarized ferromagnet<sup>12,13</sup>. Due to the Spin-Dependence of Interfacial Phase Shifts (SDIPS)<sup>14,15</sup>, one has to take into account new conduc-

tance parameters  $G_\phi^F$  and  $G_\phi^S$  at the  $F$  and  $S$  sides of the interface, respectively. It has been shown that  $G_\phi^F$  and  $G_\phi^S$  can significantly affect the behavior of  $S/F$  hybrid circuits. For instance,  $G_\phi^F$  can shift the spatial oscillations of the superconducting order parameter<sup>13</sup>. More recently, it has been found that  $G_\phi^S$  can induce an effective Zeeman splitting  $\Delta_Z^{eff}$  in a superconducting layer with a thickness  $d_S$  smaller than the superconducting coherence lengthscale  $\xi_S$ <sup>18</sup>. This induces a double gap structure (DGS) in the  $S$  and  $F$  densities of states. However, in practice, the regime  $d_S \geq \xi_S$  is frequently reached (see e.g. Refs. 19,20). Remarkably, DGSs have been recently observed at the  $F$  side of Ni/Nb bilayers with  $d_S$  much larger than  $\xi_S$ <sup>10</sup>, although Ref. 18 has found that  $\Delta_Z^{eff}$  scales with  $d_S^{-1}$  in the low  $d_S$  regime. Whether a DGS persists in the large  $d_S$  regime is therefore an important question, especially in the light of this recent experiment.

In this paper, we study how  $G_\phi^F$  and  $G_\phi^S$  modify the DOS of a  $S/F$  bilayer. We use a numerical treatment to explore a wider parameter range than in previous works. In particular, we can reach the limit of thick superconductors and larger values of  $G_\phi^S$ . We find that  $G_\phi^S$  shifts the spatial oscillations of the superconducting order parameter in  $F$ , like  $G_\phi^F$ . It can also significantly affect the amplitude of the superconducting gap. When  $d_S$  increases, the SDIPS-induced DGS becomes narrower, in agreement with Ref. 18. Nevertheless, it can surprisingly persist in the large  $d_S$  limit. Indeed, on a distance of the order of  $\xi_S$  near the  $S/F$  interface, the resonance energies of the  $S$  spectrum remain spin-dependent because quantum interferences make the superconducting correlations sensitive to the SDIPS. This behavior is transmitted to the whole  $F$  layer due to the superconducting proximity effect. We thus obtain, at the  $F$  side of  $S/F$  bilayers, DOS curves which have interesting similarities with those of Ref. 10, although  $d_S \gg \xi_S$ . More generally, our results could be useful for interpreting experiments.

This paper is organized as follows. Section II defines

the  $S/F$  bilayer problem studied in this article. Section III explains the principle of our numerical treatment. Section IV presents a detailed study of the SDIPS-induced DGS. Section V shows the effects of the SDIPS on the self-consistent superconducting gap and on the oscillations of the zero-energy DOS with the thickness of  $F$ . Section VI discusses the data of Ref. 10. Section VII concludes.

## II. DESCRIPTION OF THE $S/F$ BILAYER

We consider a diffusive  $S/F$  bilayer consisting of a standard BCS superconductor  $S$  for  $-d_S < x < 0$ , and a ferromagnet  $F$  for  $0 < x < d_F$ . We characterize the normal quasiparticle excitations and the superconducting condensate of pairs with Usadel normal and anomalous Green's functions  $G_{n,\sigma} = \text{sgn}(\omega_n) \cos(\theta_{n,\sigma})$  and  $F_{n,\sigma} = \sin(\theta_{n,\sigma})$ , with  $\theta_{n,\sigma}(x)$  the superconducting pairing angle, which depends on the spin direction  $\sigma \in \{\uparrow, \downarrow\}$ , the Matsubara frequency  $\omega_n(T) = (2n+1)\pi k_B T$ , and the spatial coordinate  $x$ <sup>21</sup>. The Usadel equations describing the spatial evolution of  $\theta_{n,\sigma}$  write

$$\xi_S^2 \frac{\partial^2 \theta_{n,\sigma}}{\partial x^2} = \frac{|\omega_n|}{\Delta_0} \sin(\theta_{n,\sigma}) - \frac{\Delta(x)}{\Delta_0} \cos(\theta_{n,\sigma}) \quad (1)$$

in  $S$  and

$$\xi_F^2 \frac{\partial^2 \theta_{n,\sigma}}{\partial x^2} = k_{n,\sigma}^2 \sin(\theta_{n,\sigma}) \quad (2)$$

in  $F$ , with

$$k_{n,\sigma} = \sqrt{2[i\sigma \text{sgn}(\omega_n) + (|\omega_n|/E_{ex})]} \quad (3)$$

In the above Eqs.,  $\Delta_0$  denotes the bulk gap of the  $S$  material,  $\xi_S = (\hbar D_S / 2\Delta_{BCS})^{1/2}$  the superconducting coherence lengthscale,  $\xi_F = (\hbar D_F / E_{ex})^{1/2}$  the magnetic coherence lengthscale,  $D_{F(S)}$  the diffusion constant in  $F(S)$  and  $E_{ex}$  the ferromagnetic exchange field of  $F$ . The self-consistent superconducting gap  $\Delta(x)$  occurring in Eq. (1) can be expressed as

$$\Delta(x) \log\left[\frac{T}{T_c}\right] = \frac{\pi k_B T}{2} \sum_{\substack{\sigma \in \{\uparrow, \downarrow\} \\ |\omega_n| \leq \Omega_D}} \left( \sin(\theta_{n,\sigma}) - \frac{\Delta(x)}{|\omega_n|} \right) \quad (4)$$

with  $\Omega_D$  the Debye frequency of  $S$ ,  $T_c^0 = \Delta_0 \exp(\mathcal{E}) / \pi k_B$  the bulk transition temperature of  $S$ ,  $k_B$  the Boltzmann constant,  $T$  the temperature and  $\mathcal{E}$  the Euler constant. The above equations must be supplemented with a description of the boundaries of  $S$  and  $F$ . We use  $\partial \theta_{n,\sigma} / \partial x|_{x=-d_S^+} = \partial \theta_{n,\sigma} / \partial x|_{x=d_F^-} = 0$  for the external sides of the bilayer. For the  $S/F$  interface, we use the spin-dependent boundary conditions<sup>12,18</sup>

$$\xi_F \frac{\partial \theta_{n,\sigma}}{\partial x} \Big|_{x=0^+} = \gamma_T \sin[\theta_{n,\sigma}^F - \theta_{n,\sigma}^S] + i\gamma_\phi^F \sigma \text{sgn}(\omega_n) \sin[\theta_{n,\sigma}^F] \quad (5)$$

and

$$\xi_S \frac{\partial \theta_{n,\sigma}}{\partial x} \Big|_{x=0^-} = \gamma_T \sin[\theta_{n,\sigma}^F - \theta_{n,\sigma}^S] - i\gamma_\phi^S \sigma \text{sgn}(\omega_n) \sin[\theta_{n,\sigma}^S] \quad (6)$$

with  $\theta_{n,\sigma}^F = \theta_{n,\sigma}(x=0^+)$  and  $\theta_{n,\sigma}^S = \theta_{n,\sigma}(x=0^-)$ . These equations involve the reduced conductances  $\gamma_T = G_T \xi_F / A \sigma_F$  and  $\gamma_\phi^{F(S)} = G_\phi^{F(S)} \xi_{F(S)} / A \sigma_{F(S)}$ , the barrier asymmetry coefficient  $\gamma = \xi_S \sigma_F / \xi_F \sigma_S$ , the normal state conductivity  $\sigma_{F(S)}$  of the  $F(S)$  material, and the junction area  $A$ . Note that we have used a definition of  $\gamma_\phi^S$  which differs from that of Ref. 18, to ensure a symmetric treatment of  $\gamma_\phi^F$  and  $\gamma_\phi^S$  in Eqs. (5-6). The microscopic expressions of the conductances  $G_T$ ,  $G_\phi^F$  and  $G_\phi^S$  can be found e.g. in Ref. 18. The term  $G_T$  corresponds to the usual tunnel conductance of the interface. The terms  $G_\phi^F$  and  $G_\phi^S$  can be finite only in case of a Spin-Dependence of Interfacial Phase Shifts (SDIPS). The SDIPS results from the fact that the scattering phases picked up by electrons upon scattering by the  $S/F$  interface can depend on spin due to the ferromagnetic exchange field or to a spin-dependent interface potential. Thus, in principle, any kind of  $S/F$  interface can have a finite SDIPS. However, the exact values of  $G_\phi^F$  and  $G_\phi^S$  are difficult to predict because they depend on the detailed microscopic structure of the interface. One possible approach is to consider  $G_\phi^F$  and  $G_\phi^S$  as fitting parameters which have to be determined from proximity effect measurements. Note that the derivation of the boundary conditions (5-6) assumes a weak transmission probability per channel (tunnel limit), which seems reasonable considering the band structure mismatch between most  $S$  and  $F$  materials. It furthermore assumes that the system is weakly polarized. However, there is no fundamental constraint on the amplitudes of  $G_T$ ,  $G_\phi^F$  and  $G_\phi^S$  because these parameters consist of a sum of contributions from numerous conducting channels.

In  $S/F$  circuits, long-range triplet correlations (between equal spins) can occur when the circuit includes several  $F$  electrodes or domains with non-collinear magnetizations<sup>22</sup>. Recently, it has been found that this effect can also arise in  $S/F$  circuits with spin-active interfaces, due to spin-flip interfacial coupling terms which are due e.g. to some misaligned local moments at the  $S/F$  interface<sup>23</sup>. In our work, we consider interfaces which are "spin-active" in the sense that the SDIPS is finite. However, we assume that there is no interfacial spin-flip coupling and that  $F$  is uniformly polarized. Hence, we don't obtain any long-range triplet component with our model.

## III. NUMERICAL TREATMENT OF THE PROBLEM

Equations (1-6) have already been solved numerically with a self-consistent procedure in the case  $\gamma_\phi^S = \gamma_\phi^F = 0$  (see e.g. Ref. 24). In this paper, we study the case of

$\gamma_\phi^S$  and  $\gamma_\phi^F$  finite, using a numerical treatment based on a relaxation method. This treatment is divided into two steps. We first calculate the values of  $\Delta(x)$  and  $\theta_{n,\sigma}$  self-consistently with a relaxation method in imaginary times. Then, we determine the pairing angle  $\theta_\sigma(\varepsilon, x)$  corresponding to the calculated  $\Delta(x)$  by using a similar relaxation method in real times, i.e. we use  $\omega_n = -i\varepsilon + \Gamma$  and  $\text{sgn}(\omega_n) = 1$  in Eqs. (1-6), with  $\varepsilon$  the energy, and  $\Gamma = 0.05\Delta_0$  a rate which accounts for inelastic processes<sup>25</sup>. Finally we obtain the DOS  $N(\varepsilon, x) = \sum_\sigma N_\sigma(\varepsilon, x)$  at position  $x$  by using  $N_\sigma(\varepsilon, x) = (N_0/2) \text{Re}[\cos[\theta_\sigma(\varepsilon, x)]]$ , with  $N_0/2$  the normal DOS per spin direction. Throughout this numerical treatment, we use a discretized space, with a step of  $0.001\xi_{S(F)}$  in  $S(F)$ . In the following, we mainly focus on  $N_F(\varepsilon) = N(\varepsilon, x = d_F^-)$ . Ref. 18 has studied analytically  $S/F$  bilayers with  $d_S \leq \xi_S/2$ ,  $\gamma_\phi^S \ll 1$ ,  $\gamma_T \ll 1$ , and  $d_F \geq \xi_F$ . Our approach allows to go beyond this regime. Note that in Figures 1 to 5, the results are shown for  $E_{ex} = 100\Delta_0$ ,  $\Omega_D = 601k_B T$  and  $k_B T = 0.1\Delta_0$ .

#### IV. THE SDIPS-INDUCED DOUBLE GAP STRUCTURE

##### A. Variations of the bilayer spectrum with the thickness of $S$

The left and right top panels of Fig. 1 show the densities of states  $N(\varepsilon, x = -d_S^+)$  and  $N(\varepsilon, x = 0^-)$  at the left and right side of the superconductor respectively, and density of states  $N_F(\varepsilon)$  at the right side of the ferromagnet (bottom panel), plotted versus  $\varepsilon$ , for different values of  $d_S$ , and the bottom panel of Fig. 1 shows the corresponding DOS  $N_F(\varepsilon)$  at the right side of  $F$ . For  $d_S = 0.35\xi_S$ , the curves calculated with our numerical code (black full lines) are in close agreement with the analytical solution given in Ref. 18 (black dashed lines). The DOS is similar at the two sides of  $S$  and displays a DGS which reveals the existence of an effective Zeeman splitting of the form

$$\Delta_Z^{eff} = 2\Delta_0 \frac{\xi_S}{d_S} \gamma_\phi^S = E_{TH}^S \frac{G_\phi^S}{G_S} \quad (7)$$

with  $E_{TH}^S = \hbar D_S/d_S^2$  the Thouless energy of the  $S$  layer and  $G_S = \sigma_S A/d_S$  its normal state conductance. The DGS is also visible in  $N_F(\varepsilon)$  due to the proximity effect. It becomes narrower when  $d_S$  increases, in agreement with Eq. (7) which indicates that  $\Delta_Z^{eff}$  scales with  $d_S^{-1}$ . For very large values of  $d_S$ , the DOS  $N(\varepsilon, x = -d_S^+)$  at the left side of  $S$  tends to the bulk value  $\text{Re}(\cos(\theta_0(\varepsilon)))$ , with  $\theta_0(\varepsilon) = \arctan(\Delta_0/(-i\varepsilon + \Gamma))$  (see top left panel, blue full line). However, a DGS remains clearly visible in  $N_F(\varepsilon)$ , a result which is quite counterintuitive considering the low  $d_S$  expression Eq. (7) (see bottom panel, blue full line). Note that in the  $S$  layer, with the parameters of Fig. 1,  $d_S \gg \xi_S$  and  $\varepsilon = 0$  [ $\varepsilon = \Delta_0$ ],  $N(\varepsilon, x)$  decays from its bulk value to  $N(\varepsilon, x = 0^-)$  on a distance of the order of  $\xi_S$  [ $2\xi_S$ ] near the interface (not shown). In the large

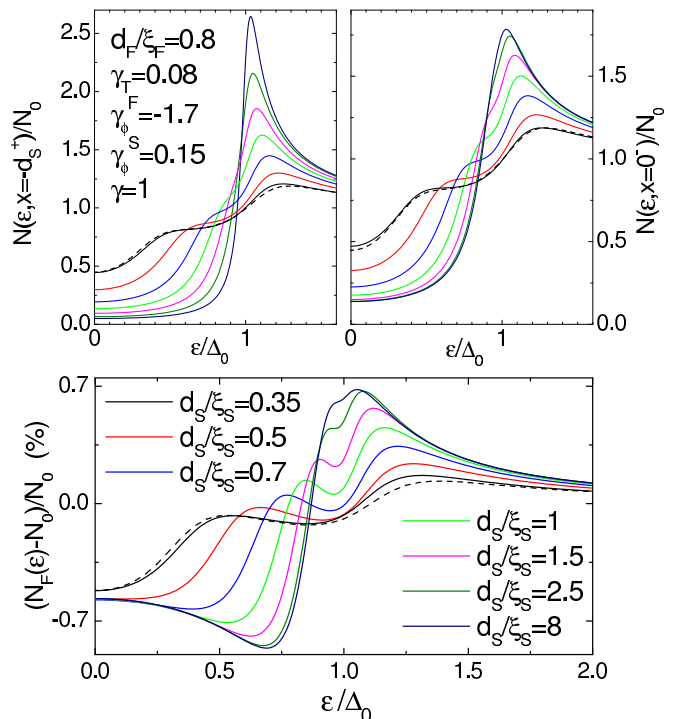


FIG. 1: Densities of states  $N(\varepsilon, x = -d_S^+)$  (top left panel) and  $N(\varepsilon, x = 0^-)$  (top right panel) at the left and right side of the superconductor respectively, and density of states  $N_F(\varepsilon)$  at the right side of the ferromagnet (bottom panel), plotted versus  $\varepsilon$ , for different values of  $d_S$ . The full lines correspond to our numerical results. The black dashed lines correspond to the analytical predictions of Ref. 18, for  $d_S/\xi_S = 0.35$ .

$d_S$  limit, the DOS  $N(\varepsilon, x = 0^-)$  at the left side of the  $S/F$  interface does not show a clear DGS for the weak value of  $\gamma_\phi^S$  used in Fig. 1, because of the strong DOS peak at  $\varepsilon = \Delta_0$  (see top right panel, blue full line). However, a DGS would appear more clearly in  $N(\varepsilon, x = 0^-)$  for larger values of  $\gamma_\phi^S$ , e.g. using  $\gamma_\phi^S = 0.4$  (not shown). The DGS thus seems to persist at large values of  $d_S$  due to an effect which involves a  $S$  area with thickness  $\sim \xi_S$  near the  $S/F$  interface and the whole  $F$ .

##### B. Variations the bilayer spectrum with the thickness of $F$

Due to the ferromagnetic exchange field  $E_{ex}$ , the zero-energy DOS  $N_F(\varepsilon = 0)$  oscillates around its normal state value  $N_0$  when  $d_F$  increases<sup>6,26,27,28</sup>. In the large  $d_S$  limit, we find that the DGS can occur at the  $F$  side for both an ordinary ( $N_F(\varepsilon = 0) > N_0$ ) and a reversed ( $N_F(\varepsilon = 0) < N_0$ ) DOS. However, its visibility varies with  $d_F$ , like in the limit  $d_S \leq \xi_S/2$  of Ref. 18. Figure 2, left panel, shows  $N_F$  versus  $\varepsilon$ , for different values of  $d_F$  and  $d_S/\xi_S = 5$ . From  $d_F = 0.53\xi_F$  to  $0.58\xi_F$ ,  $N_F(\varepsilon = 0) - N_0$  is positive and the visibility of the DGS increases (see black, blue and green full lines). For

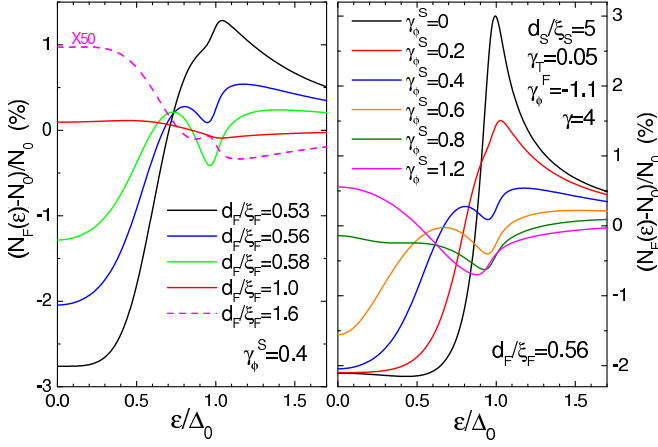


FIG. 2: Density of states  $N_F(\varepsilon)$  at the right side of the ferromagnet, plotted versus  $\varepsilon$ , for different values of  $d_F$  (left panel) and different values of  $\gamma_\phi^S$  (right panel). In the left panel, for  $d_F/\xi_F = 1.6$ , we have multiplied  $(N_F(\varepsilon) - N_0)/N_0$  by a factor 50 for visibility of the curve.

$d_F = \xi_F$ ,  $N_F(\varepsilon = 0) - N_0$  is negative and the DGS is not visible anymore (see red full line). For  $d_F = 1.6\xi_F$ , the DGS is visible again, with both the inner and outer peaks of the DOS inverted due to  $N_F(\varepsilon = 0) - N_0 < 0$  (see pink dashed line).

### C. Variations of the bilayer spectrum with $G_\phi^S$

In the parameters range investigated by us (with in particular  $E_{ex} \gg \Delta$ ,  $0.35 \leq d_S/\xi_S \leq 10$  and  $0.4 \leq d_F/\xi_F \leq 4$ ), no DGS occurs when  $\gamma_\phi^S = 0$ . The DGS studied in this article thus seems to be a direct consequence of  $\gamma_\phi^S \neq 0$  for  $d_S/\xi_S$  large as well as  $d_S/\xi_S$  small. Figure 2, right panel, shows the variations of  $N_F(\varepsilon)$  with  $\gamma_\phi^S$ , for a constant value of  $d_F$ . For  $\gamma_\phi^S = 0$ , no DGS appears. For a very small  $\gamma_\phi^S$  (see red full line, corresponding to  $\gamma_\phi^S = 0.2$  or  $G_\phi^S = G_T$ ),  $N_F(\varepsilon)$  shows a change of slope which corresponds to a smoothed DGS, near  $\varepsilon = \Delta_0$  (from the previous section, this DGS occurs only for certain values of  $d_F$ ). When  $\gamma_\phi^S$  becomes sufficiently large,  $N_F(\varepsilon)$  shows a clear DGS, i.e. two peaks, one above and one below  $\varepsilon = \Delta_0$ , while a local minimum is visible for  $\varepsilon \sim \Delta_0$ . The distance between the two peaks of  $N_F(\varepsilon)$  increases with  $\gamma_\phi^S$ . In Fig. 2, when  $\gamma_\phi^S$  becomes too large ( $\gamma_\phi^S \geq 0.8$ ), the sign of  $N_F(\varepsilon = 0) - N_0$  changes. This suggests that  $\gamma_\phi^S$  does not only induce DGSs but also shifts the oscillations of  $N_F(\varepsilon)$  with  $d_F$ . This last effect will be investigated in more details for  $\varepsilon = 0$  in section V. With the parameters of Fig. 2, the DGS is not visible anymore when  $\gamma_\phi^S$  becomes larger than approximately 1. In the general case, this threshold strongly depends on the different parameters characterizing the  $S/F$  bilayer.

### D. Analytic description of the thick superconductor limit

In order to have a better insight on the persistence of the SDIPS-induced DGS at large values of  $d_S$ , we provide in this section an analytic description of the case where  $S$  is semi-infinite. For simplicity, we assume that the superconducting gap is only weakly affected by the presence of the  $F$  layer, i.e.  $\Delta(x) = \Delta_0$ . We furthermore assume that the proximity effect is weak, i.e.  $\theta_{n,\sigma}(x \in F) \ll 1$  and  $\theta_{n,\sigma}(x \in S) - \theta_n^0 \ll 1$ , with  $\theta_n^0 = \arctan(\Delta_0/|\omega_n|)$ . In this case, the Usadel Eqs. (1-2) lead to:

$$\theta_{n,\sigma}(x) = \theta_{n,\sigma}^F \cosh\left(\frac{[x - d_F]k_{n,\sigma}}{\xi_F}\right) / \cosh\left(\frac{d_F k_{n,\sigma}}{\xi_F}\right) \quad (8)$$

for  $x \in F$  and

$$\theta_{n,\sigma}(x) = \theta_n^0 + \delta\theta_{n,\sigma}^S \exp\left(\frac{x\eta_n}{\xi_S}\right) \quad (9)$$

for  $x \in S$ , with  $\eta_n = (1 + (\omega_n/\Delta_0)^2)^{1/4}$ . We have introduced in the above Eqs.  $\delta\theta_{n,\sigma}^S = \theta_{n,\sigma}(x = 0^-) - \theta_n^0$  and  $\theta_{n,\sigma}^F = \theta_{n,\sigma}(x = 0^+)$ . The linearization of the boundary conditions (5-6) with respect to these two quantities leads to:

$$\theta_{n,\sigma}^F = \frac{\gamma_T (\sin(\theta_n^0) + \cos(\theta_n^0)\delta\theta_\sigma^S)}{\gamma_T \cos(\theta_n^0) + i\gamma_\phi^F \sigma \text{sgn}(\omega_n) + B_{n,\sigma}} \quad (10)$$

and

$$\delta\theta_{n,\sigma}^S = -\frac{\gamma\gamma_T + i\gamma_\phi^S \sigma \text{sgn}(\omega_n)}{\eta_n^3 + [\gamma\gamma_T + i\gamma_\phi^S \sigma \text{sgn}(\omega_n)] \frac{|\omega_n|}{\Delta_0}} \quad (11)$$

with  $B_{n,\sigma} = k_{n,\sigma} \tanh[d_F k_{n,\sigma}/\xi_F]$ . Importantly, Eqs. (8-11) are valid provided  $\delta\theta_{n,\sigma}^S \ll 1$  and  $\theta_{n,\sigma}^F \ll 1$ , which requires  $\gamma_T \ll 1$ ,  $\gamma_\phi^S \ll 1$  and  $d_F \geq \xi_F$ . We have used these hypotheses to simplify Eq. (11). The validity of the approximation  $\Delta(x) = \Delta_0$  will be discussed in section V.

Figure 3 shows  $N_F(\varepsilon)$  calculated from the analytic continuation of Eqs. (8-11) (black dashed lines) and from our numerical code (red full lines), for a weak value of  $\gamma$ , and  $\gamma_\phi^S = 0$  (left panel) or  $\gamma_\phi^S \neq 0$  (right panel). The two calculations are in relatively good agreement<sup>29</sup>. For the parameters used in Fig. 3, we have checked numerically that the approximation  $\Delta(x) = \Delta_0$  gives results in very good agreement with the full resolution of Eqs. (1-6). At  $\varepsilon \sim \Delta_0$ , small discrepancies arise between the predictions of the numerical code and of Eqs. (8-11), due to resonance effects which make  $\delta\theta_{n,\sigma}^S$  and  $\theta_{n,\sigma}^F$  larger than for  $\varepsilon = 0$  or  $\varepsilon \gg \Delta_0$ . Equations (8-11) allow to recover the fact that a DGS can appear in  $N_F(\varepsilon)$ , due to  $\gamma_\phi^S \neq 0$  (right panel). In the limit  $d_S \gg \xi_S$ , the pairing angle of the system cannot be put under the form  $\theta_\sigma(x, \varepsilon) = \theta(x, \varepsilon - [\sigma\Delta_Z^{eff}/2])$ ,

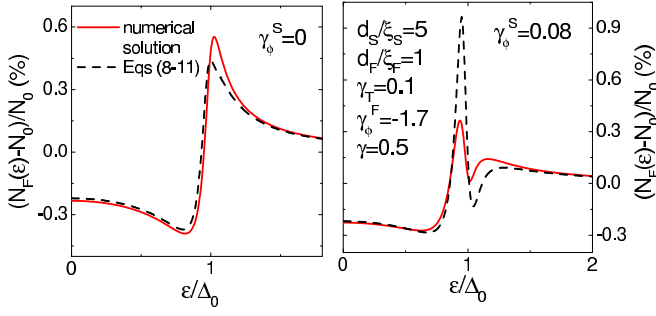


FIG. 3: Density of states  $N_F(\epsilon)$  at the right side of the ferromagnet, plotted versus  $\epsilon$ , for  $\gamma_\phi^S = 0$  (left panel) and  $\gamma_\phi^S$  finite (right panel). The red lines are calculated from Eqs. (8-11) and the black dotted lines correspond to the self-consistent numerical resolution of Eqs. (1-6).

contrarily to what has been found for  $d_S \leq \xi_S/2$ . Therefore, the notion of SDIPS-induced effective Zeeman splitting is not valid for thick  $S$  layers. Nevertheless, from Eqs. (9,11), near the  $S/F$  interface, the resonance energies of the  $S$  spectrum can be spin-dependent because quantum interferences make the superconducting correlations sensitive to the SDIPS on a distance of the order of  $\xi_S/\eta_m$  near the  $S/F$  interface. From Eqs. (8,10), this behavior is transmitted to the whole  $F$  layer due to the proximity effect. From Eq. (11), the energy scale related to the occurrence of the DGS has the form:

$$\Delta_{SDIPS} = 2\Delta_0 \frac{\widetilde{G}_\phi^S}{G_S} \quad (12)$$

with  $\widetilde{G}_S = \sigma_S A/\xi_S$  the normal state conductance of a slab of thickness  $\xi_S$  of the  $S$  material. Interestingly, this expression has a form similar to Eq. (7), with  $d_S$  replaced by  $\xi_S$  (one has  $2\Delta_0 = \hbar D_S/\xi_S^2 = E_{TH}^S$ ). Note that for a ballistic  $S/F$  single channel contact, the SDIPS also produces a spin-dependent resonance effect<sup>30</sup>. However, in this case, one does not obtain a DGS but rather a sub-gap resonance in the conductance and the zero-frequency noise of the system.

## V. SELF-CONSISTENT SUPERCONDUCTING GAP AND ZERO-ENERGY DOS OF $F$

For completeness, we now discuss the effects of the SDIPS on the self-consistent superconducting gap  $\Delta(x)$  and the zero-energy DOS  $N_F(\epsilon = 0)$  versus  $d_F$ .

It is already known that the amplitude of  $\Delta(x)$  decreases when  $\gamma_T$  or  $\gamma$  increase, similarly to what happens in a  $S$ /normal metal bilayer<sup>31</sup>. Figure 4 compares the effects of  $\gamma$  (left panel) and  $\gamma_\phi^S$  (right panel) on  $\Delta(x)$  (it only shows the effect of  $\gamma_\phi^S > 0$ , but the effect of  $\gamma_\phi^S < 0$  is similar). One can see that  $\Delta(x)$  significantly decreases when  $|\gamma_\phi^S|$  increases. Similarly, in a clean superconductor connected to a ferromagnetic insulator ( $FI$ ),  $\Delta(x)$  has

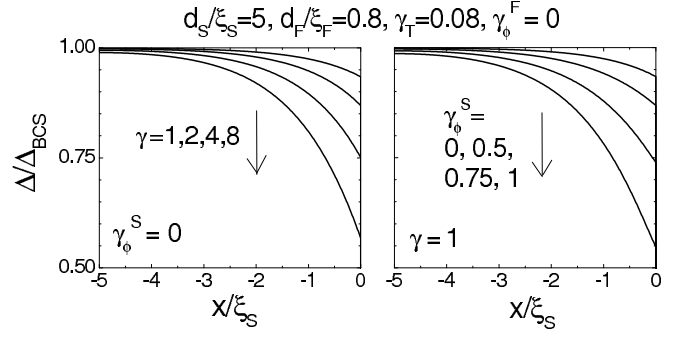


FIG. 4: Self-consistent superconducting gap  $\Delta(x)$  versus the spatial coordinate  $x$ , for different values of  $\gamma$  (left panel) and  $\gamma_\phi^S$  (right panel).

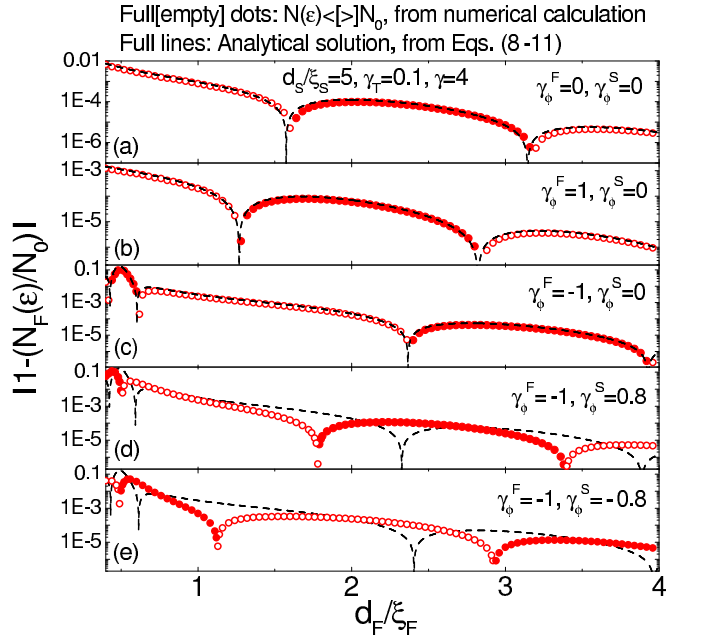


FIG. 5: Zero-energy density of states  $N_F(\epsilon = 0)$  at the right side of  $F$ , versus the thickness  $d_F$  of  $F$ . The density of states calculated numerically is shown with red dots. The full and empty dots correspond to  $N_F(\epsilon = 0) < 0$  and  $N_F(\epsilon = 0) > 0$ , respectively. The density of states given by Eqs. (8-11) is shown with black dashed lines. Panel (a) corresponds to a case with no SDIPS ( $\gamma_\phi^F = \gamma_\phi^S = 0$ ). Panels (b) and (c) show the effect of a finite  $\gamma_\phi^F$ . Panels (d) and (e) show the effect of a finite  $\gamma_\phi^S$ , in comparison with panel (c) where  $\gamma_\phi^S = 0$ . With the parameters used here, Eqs. (8-11) are in agreement with our numerical code only when  $\gamma_\phi^S = 0$ .

been predicted to decrease due to the spin-dependence of the reflection phases against  $FI$ <sup>17</sup>. In contrast, in the regime of parameters investigated by us,  $\gamma_\phi^F$  has a negligible effect on the value of  $\Delta(x)$  because it does not occur directly in the boundary condition (11) at the  $S$  side of the interface. From this brief study of  $\Delta(x)$ , we conclude that the approximation  $\Delta(x) = \Delta_0$  used in section IV D is valid only for sufficiently small values of  $\gamma_T$ ,  $\gamma$  and  $\gamma_\phi^S$ .

Figure 5 presents the effects of  $\gamma_\phi^F$  and  $\gamma_\phi^S$  on the variations of  $N_F(\varepsilon = 0)$  with  $d_F$ . The DOS calculated numerically is shown with symbols and the DOS given by Eqs. (8-11) is shown with full lines. In panels (a), (b) and (c), we have used  $\gamma_\phi^S = 0$ , so that the two calculations are in close agreement. In panels (d) and (e), the two calculations strongly differ because  $\gamma_\phi^S$  is too large for the hypotheses leading to Eqs. (8-11) to be valid. We recover the fact that, in the regime  $d_F \geq \xi_F$ ,  $N_F(\varepsilon = 0)$  shows exponentially damped oscillations with  $d_F$ <sup>6,26</sup>. In the regime  $d_F \leq \xi_F$ , the oscillations of  $N_F(\varepsilon = 0)$  with  $d_F$  are less regular. This can be understood from the analytic description of Section IV D. For  $d_F \geq \xi_F$ , one has  $B_{n,\sigma} \sim k_{n,\sigma}$ , so that  $N_F(\varepsilon = 0)$  depends on  $d_F$  through the  $\cosh(d_F k_{n,\sigma}/\xi_F)$  term of Eq. (8) only. For  $d_F \leq \xi_F$ ,  $B_{n,\sigma}$  and thus  $\theta_{n,\sigma}^F$  strongly depend on  $d_F$ , which complicates the variations of  $N_F(\varepsilon = 0)$  with  $d_F$  and leads to more irregular oscillations. Ref. 13 has already shown that  $\gamma_\phi^F$  can shift the oscillations of  $N_F(\varepsilon = 0)$  with  $d_F$ . Panels (b) and (c) confirm this result and also shows that a positive (negative)  $\gamma_\phi^F$  decreases (increases) the amplitude of  $N_F(\varepsilon = 0)$ . From panels (d) and (e),  $\gamma_\phi^S$  can also significantly shift the oscillations of  $N_F(\varepsilon = 0)$  with  $d_F$ , in agreement with Fig. 2, right panel. For the parameters used in Fig. 5,  $\gamma_\phi^S$  does not modify spectacularly the amplitude of  $N_F(\varepsilon)$ . For larger values of  $|\gamma_\phi^S|$ , the amplitude of the superconducting proximity effect would significantly decrease due to a reduction of  $\Delta(x)$  (not shown).

## VI. DISCUSSION ON THE DATA OF PHYS. REV. LETT. 100, 237002 (2008)

We now consider the DOS measurements realized by SanGiorgio et al. for Nb/Ni bilayers with  $d_S = 50$  nm<sup>10</sup>. From Ref. 19 which considers samples fabricated by the same team, one has  $\xi_S \sim 10$  nm, so that  $d_S/\xi_S \sim 5$ . However, double gap structures have been observed by SanGiorgio et al., which motivates a comparison with our model.

Figure 6 compares the data measured for  $d_F = 1.5$  nm (black squares) with our numerical calculation (blue full line). Our calculation reproduces almost quantitatively the experimental curve. We have used  $d_F = 1.5$  nm,  $d_S/\xi_S = 5$  and  $T = 280$  mK, in agreement with Refs. 10,19. We have also used the exchange field  $E_{ex} = 78$  meV, estimated by Ref. 10, and the Debye temperature  $T_D = 275$  K of Nb, taken from Ref. 32. We have assumed  $\xi_F = 2.83$  nm,  $\gamma_T = 0.06$ ,  $\gamma_\phi^F = -1.1$ ,  $\gamma_\phi^S = 0.5$ , and  $\Gamma = 0.025\Delta_0$ . Note that from Ref. 19, one has  $\sigma_S^{-1} \sim 15.9$   $\mu\Omega$ .cm and  $\sigma_F^{-1} \sim 9.7$   $\mu\Omega$ .cm, so that one should have  $\gamma = \xi_S\sigma_F/\xi_F\sigma_S \sim 2.9$  with the above values of  $\xi_S$  and  $\xi_F$ . In Figure 6, we have used a value  $\gamma = 2$ , which is in relatively good agreement with this estimate. The values of  $\gamma_T$ ,  $\gamma_\phi^F$ ,  $\gamma_\phi^S$  and  $\gamma$  used in the fit yield  $G_\phi^F/G_T \sim 18$  and  $G_\phi^S/G_T \sim 4$ . A theoretical

prediction of these ratios is very difficult because they depend on the detailed microscopic structure of the Nb/Ni interface. However, with a simple delta function barrier model, it already is possible to find situations where  $G_\phi^S$  and  $G_\phi^F$  are larger than  $G_T$  (see Appendix A and Fig. 6 of Ref. 18). Therefore, we think that the SDIPS parameters used by us are possible.

We cannot reproduce quantitatively the data obtained by SanGiorgio et al. for all values of  $d_F$  with the same set of parameters as for  $d_F = 1.5$  nm. We think that this might be due to the fact that some characteristics of the samples like e.g.  $E_{ex}$  and thus  $\xi_F$ ,  $\gamma_\phi^F$ ,  $\gamma_\phi^S$ , and  $\gamma$  can vary with  $d_F$ <sup>33</sup>. In the data of SanGiorgio et al., from  $d_F = 1.5$  nm to  $d_F = 3.0$  nm, the distance between the two peaks of the DGS increases, like in our model (see Fig. 2, left panel). However, the outer peak of the DGS remains very close to  $\varepsilon \sim \Delta_0$ , which seems difficult to reproduce with our model. Note that in Ref. 10, for  $d_F = 3.5$  nm, the outer peaks of the DOS are inverted, whereas a sharp dip occurs at low energies, which can give the impression that the inner peaks of the DOS persist but are not inverted, in contrast to what we find (see section IV.B). However, we think that the observation of this zero-bias dip is not totally reliable. Indeed, SanGiorgio et al. explain that, in the DOS of their thickest samples (for  $d_F > 3.5$  nm), "the zero bias peak is due to the steep voltage dependence of the background conductance and is therefore a by-product of the data normalization procedure". The zero bias-dip of the  $d_F = 3.5$  nm sample occurs on the same energy scale as these zero-bias peaks, and it goes together with a strange zero-bias singularity similar to those shown by the thickest samples. Therefore, we are not sure whether a proper interpretation of the data of Ref. 10 must take into account this feature. Ref. 34 suggests that the DGS observed by Sangiorgio could be due to triplet correlations. However, it is difficult to know whether this interpretation can be more satisfying than ours because Ref. 34 does not shown any quantitative interpretation of the data and does not discuss, for instance, the evolution of the inner and outer peak positions with  $d_F$ .

## VII. CONCLUSION

In summary, we have calculated the density of states (DOS) in a diffusive superconducting/ferromagnetic (S/F) bilayer with a spin-active interface. We have used a self-consistent numerical treatment to make a systematic study of the effects of the Spin-Dependence of Interfacial Phase Shifts (SDIPS). We characterize the SDIPS with two conductance-like parameters  $G_\phi^S$  and  $G_\phi^F$ , which occur in the boundary conditions describing the  $S$  and  $F$  sides of the interface, respectively. We find that the amplitude of  $\Delta(x)$  significantly decreases if  $G_\phi^S$  is too strong, whereas it is almost insensitive to  $G_\phi^F$ . In contrast, both  $G_\phi^S$  and  $G_\phi^F$  can shift the oscillations of the

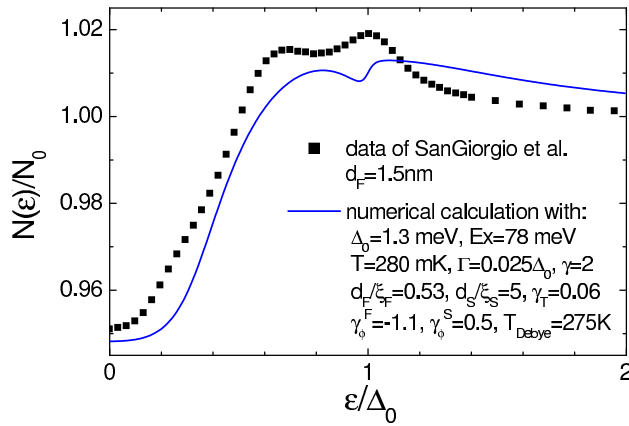


FIG. 6: Comparison between the data of SanGiorgio et al., Phys. Rev. Lett. **100**, 237002 (2008), for  $d_s = 1.5$  nm, and our numerical calculation with  $\Delta_0 = 1.3$  meV,  $E_{ex} = 78$  meV,  $k_B T = 280$  mK,  $d_F/\xi_F = 0.53$ ,  $d_S/\xi_S = 5$ ,  $\gamma_T = 0.06$ ,  $\gamma_\phi^F = -1.1$ ,  $\gamma_\phi^S = 0.5$ ,  $\gamma = 2$ ,  $T_{Debye} = 275$  K and  $\Gamma = 0.025\Delta_0$ .

zero-energy DOS of  $F$  with the thickness of  $F$ . Remarkably, we find that the SDIPS can produce a double gap structure in the DOS of  $F$ , even when the  $S$  layer is much thicker than the superconducting coherence length. This leads to DOS curves which have striking similarities with those of Ref. 13. More generally, our results could be useful for interpreting future experiments on superconducting/ferromagnetic diffusive hybrid structures.

We acknowledge interesting discussions with A. A. Golubov, T. Kontos, M. Yu. Kuprianov and N. Regnault. We thank P. SanGiorgio and M. Beasley for discussions and for sending us their data. J.L. was supported by the Research Council of Norway, Grants No.158518/431 and No. 158547/431 (NANOMAT), and Grant No. 167498/V30 (STORFORSK).

- <sup>1</sup> A. A. Golubov, M. Yu. Kuprianov, and E. Il'ichev, Rev. Mod. Phys. **76**, 411 (2004).
- <sup>2</sup> A. I. Buzdin, Rev. Mod. Phys. **77**, 935 (2005).
- <sup>3</sup> W. Guichard, M. Aprili, O. Bourgeois, T. Kontos, J. Lesueur, and P. Gandit, Phys. Rev. Lett. **90**, 167001 (2003).
- <sup>4</sup> L. B. Ioffe, V. B. Geshkenbein, M. V. Feigel'man, A. L. Fauchère, G. Blatter, Nature **398**, 679 (1999).
- <sup>5</sup> T. Yamashita, K. Tanikawa, S. Takahashi and S. Maekawa, Phys. Rev. Lett. **95**, 097001 (2005).
- <sup>6</sup> T. Kontos, M. Aprili, J. Lesueur, and X. Grison, Phys. Rev. Lett. **86**, 304 (2001).
- <sup>7</sup> T. Kontos, M. Aprili, J. Lesueur, X. Grison, and L. Dumoulin, Phys. Rev. Lett. **93**, 137001 (2004).
- <sup>8</sup> L. Crétonin, A. K. Gupta, H. Sellier, F. Lefloch, M. Fauré, A. Buzdin, and H. Courtois, Phys. Rev. B **72**, 024511 (2005).
- <sup>9</sup> S. Reymond, P. SanGiorgio, M. R. Beasley, J. Kim, T. Kim, and K. Char, Phys. Rev. B **73**, 054505 (2006).
- <sup>10</sup> P. SanGiorgio, S. Reymond, M. R. Beasley, J. H. Kwon, and K. Char, Phys. Rev. Lett. **100**, 237002 (2008).
- <sup>11</sup> M. Yu. Kuprianov and V. F. Lukichev, JETP **67**, 1163 (1988).
- <sup>12</sup> D. Huertas-Hernando, Yu. V. Nazarov, and W. Belzig, cond-mat/0204116; D. Huertas-Hernando, Phd Thesis, Delft University of Technology, The Netherlands (2002), D. Huertas Hernandez, Yu. V. Nazarov, and W. Belzig, Phys. Rev. Lett. **88**, 047003 (2002).
- <sup>13</sup> A. Cottet and W. Belzig, Phys. Rev. B **72**, 180503(R) (2005).
- <sup>14</sup> The SDIPS is called by some other authors "spin-mixing angle" or "spin-rotation angle". However, in our case, we consider a single ferromagnet which is uniformly polarized, so that the notions of mixing or rotation are not relevant.
- <sup>15</sup> The effects of the SDIPS on  $S/F$  systems have been initially studied in the ballistic case, see e.g. Refs. 16,17.
- <sup>16</sup> A. Millis, D. Rainer, and J. A. Sauls, Phys. Rev. B **38**, 4504 (1988).
- <sup>17</sup> T. Tokuyasu, J. A. Sauls and D. Rainer, Phys. Rev. B **38**, 8823 (1988).
- <sup>18</sup> A. Cottet, Phys. Rev. B **76**, 224505 (2007).
- <sup>19</sup> J. Kim, J. H. Kwon, K. Char, H. Doh, and H.-Y. Choi, Phys. Rev. B **72**, 014518 (2005).
- <sup>20</sup> Th. Mühge, K. Westerholt, H. Zabel, N. N. Garif'yanov, Yu. V. Goryunov, I. A. Garifullin, and G. G. Khaliullin, Phys. Rev. B **55**, 8945 (1997).
- <sup>21</sup> N. B. Kopnin, Theory of Nonequilibrium Superconductivity, Clarendon Press, Oxford (2001); W. Belzig, F. K. Wilhelm, C. Bruder, G. Schön and A. D. Zaikin, Superlatt. and Microstr. **25**, 1251 (1999).
- <sup>22</sup> F. S. Bergeret, A. F. Volkov, and K. B. Efetov, Rev. Mod. Phys. **77**, 1321 (2005).
- <sup>23</sup> M. Eschrig, J. Kopu, J. C. Cuevas, and Gerd Schön, Phys. Rev. Lett. **90**, 137003 (2003); Y. Asano, Y. Sawa, Y. Tanaka, and A. A. Golubov, Phys. Rev. B **76**, 224525 (2007); A. V. Galaktionov and M.S. Kalenkov, I.E. Tamm, A. D. Zaikin, Phys. Rev. B **77**, 094520 (2008); M. Eschrig, T. Lofwander, Nature Phys. **4**, 138 (2008).
- <sup>24</sup> D. Yu. Gusakova, A. A. Golubov, M. Yu. Kuprianov, A. Buzdin, JETP letters **83**, 327 (2006).
- <sup>25</sup> W. Belzig, PhD thesis, Karlsruhe university (1999).
- <sup>26</sup> A. Buzdin, Phys. Rev. B **62**, 11377 (2000), I. Baladié and A. Buzdin, Phys. Rev. B **64**, 224514 (2001).
- <sup>27</sup> M. Zareyan, W. Belzig, and Yu. V. Nazarov, Phys. Rev. Lett. **86**, 308 (2001); Phys. Rev. B **65**, 184505 (2002).
- <sup>28</sup> F. S. Bergeret, A. F. Volkov, and K. B. Efetov, Phys. Rev. B **65**, 134505 (2002).
- <sup>29</sup> For the parameters of Figs. 1 and 2, Equations (8-11) are not in good agreement with our numerical results because the hypotheses leading to these equations are not satisfied (see section V.)
- <sup>30</sup> A. Cottet and W. Belzig, Phys. Rev. B **77**, 064517 (2008).
- <sup>31</sup> A. A. Golubov and M. Yu. Kuprianov, Sov. Phys. JETP **69**, 805 (1990).
- <sup>32</sup> N. W. Ashcroft and N. D. Mermin, Solid State Physics (Saunders College Publishing, Philadelphia, 1976).

- <sup>33</sup> T. Kontos, Ph.D. thesis, Université Paris-Sud, Orsay, France, 2002. (2008).
- <sup>34</sup> A. F. Volkov and K. B. Efetov, Phys. Rev. B **78**, 024519